CHARACTERIZATION OF A COLD PLATE BY EXPERIMENTAL ANALYSIS AND POWER SAVINGS CALCULATION OF DYNAMIC COLD PLATE

By

BARATH RAGUL MANIMARAN

Presented to the Faculty of the Graduate School of
The University of Texas at Arlington in Partial Fulfillment
Of the Requirements
for the Degree of

MASTER OF SCIENCE IN MECHANICAL ENGINEERING

THE UNIVERSITY OF TEXAS AT ARLINGTON

May 2018

Acknowledgements

Thanks to God Almighty for giving me the strength and wisdom to understand, learn and complete this research.

I would like to take this opportunity to express my deep gratitude to my supervising professor Dr. Dereje Agonafer for his encouragement, support and guidance during my research work at The University of Texas at Arlington. He is primarily responsible for encouraging me to take up this project and helping me expand my network through conferences and workshops.

I would also like to thank Dr. Haji-Sheikh and Dr. Andrey Beyle for serving on my dissertation committee. I owe a great deal of gratitude to Dr. Steve from Asetek Inc. for providing me with the resources such as the cold plates for my research work. Special thanks to Dr. John Fernandes and Mark Seymour and all the mentors who helped me throughout the research work. A special thanks to Mr. Rajesh Kasukurthy and Rishi Ruben for helping me out throughout the project.

I cannot thank Ms. Fatima Ayesha for her assistance with administrative matters during my time with the EMNSPC. Our conversations always served as a stress reliever and her concern for my well-being was genuine. I would also like to thank all the Mechanical and Aerospace Engineering Department faculty and staff that supported me throughout my graduate studies and helped me get through it all.

Last, but not the least, I would like to thank my dear dad (Manimaran Mannangatty), mom (Geetha Manimaran) and my elder brother (Dinesh Gokul Manimaran), Stephna and my friends for believing in me to achieve success in all my endeavors. I would not be the man I am today if it is not for their unconditional love and support.

April 27, 2018

Abstract

CHARACTERIZATION OF A COLD PLATE BY EXPERIMENTAL ANALYSIS AND POWER SAVINGS CALCULATION OF DYNAMIC COLD PLATE

Barath Ragul Manimaran, MS

The University of Texas at Arlington, 2018

Supervising Professor: Dr. Dereje Agonafer

Cooling is a critical part of data center's infrastructure, and with ongoing demands in data processing and storage, thermal management issues are of great concern. Some imperative methods of removing heat are either using air or liquid (preferably water or refrigerant). When high power densities modules are involved, liquid cooling addresses some of the problems faced by air cooling as liquid coolants have higher thermal capacitance. Also, in the case of multi-chip modules, a non-uniform heating due to multicore generates hotspots and increases temperature gradients across the module. A dynamic cold plate was developed to address these issues with the help of flow control devices. A temperature sensing self-regulated flow control device (FCD) is placed at the exit of each section to regulate the required flow. This thesis presents an experimental setup with two 240W heat sources cooled by Asetek cold plates connected in parallel to each other. The Performance characteristics of the Asetek cold plate is comprehensively studied by experimental testing. In addition to the experimental study, the computational results from the FCD are studied to estimate pumping power savings.

Table of Contents

List of Illustrations

List of Tables

Chapter 1

Introduction

Data centers are facilities used to store, organize, process and access data and comprises a network of computers and other relevant components. Power supplies, communication and storage equipment, fire suppression equipment, heating ventilation and air conditioning (HVAC) equipment and monitoring systems are the components used in a data center. Data storage and data sharing has become vital in the growth of all industries. Due to the massive increase in usage of datacenters, the storage and sharing of data are happening globally.

Architecture and requirements of data centers vary significantly. For example, a data center built for a cloud service provider like Amazon® EC2 satisfies facility, infrastructure, and security requirements that significantly differ from a completely private data center, such as one built for the Pentagon that is dedicated to securing classified data.

An optimized data center operation is often characterized by a well-balanced investment of facility and equipment. The elements that constitute a data center are as follows:

Facility- the location and “white space”, i.e., the usable space available for the use of IT equipment. Data Centers are often considered as one of the most power consuming facilities existing, as they are accessed y the end users round-the-clock. Therefore, optimization of white-space and controlling the humidity and temperature of the data centers environment, within the specifications of the manufacturer is imperative for the efficiency of data centers.

Support infrastructure – equipment tha enables the highest availability of data. The Uptime Institute has defined four tiers of data centers, with availability ranging from 99.671% to 99.995%. Some components for supporting infrastructure include:

- Uninterruptible Power Sources (UPS) – battery banks, generators and redundant power sources.
- Environmental Control – computer room air conditioners (CRAC), heating, ventilation, and air conditioning (HVAC) systems, and exhaust systems.
- Physical Security Systems – biometrics and video surveillance systems.

IT equipment – equipment used for IT operations and storage of the organization's data, such as the servers, storage hardware, cables, racks and firewall equipments.

Operations staff – man power required to monitor and maintain the operations and infrastructure required.

In the recent years, technologies like virtualization are utilized in data centers in order to optimize resource utilization and also to increase flexibility of data. As firms are in a need to continuously evolve towards the on-demand services, firms have shifted to cloud basaed computing and infrastructure. This demand has led to a focus on making the data centers more energy efficient, known as 'green data centers', by following technologies and practices to reduce the energy consumption. This paper is an effort to one such initiative.

Figure 1-1 Data Center [1]

With the increase in packaging densities of the electronics components, Cooling of electronics is becoming more challenging. A more recent concern is the low efficiency in air-based data center cooling technologies. One efficient way to cool the electronic components is by Liquid Cooling because of the high heat transfer coefficients achieved compared to the conventional air cooling. Figure 1-2 shows a typical data center server rack with a liquid to liquid heat exchanger sits on top of it. Incorporating this setup helps in eliminating the need for chillers and the CRACs. Air is commonly used as cooling medium for many devices. For devices with dynamic cooling air can't play an effective role. So, liquids became viable replacement with its high thermal properties. Liquid became very efficient for an optimized cooling, a variety of liquids used as coolants are listed in Table1-1. Among liquids, water became most usable cooling medium because of its high thermal conductivity and abundant availability. So, water became successful cooling medium.

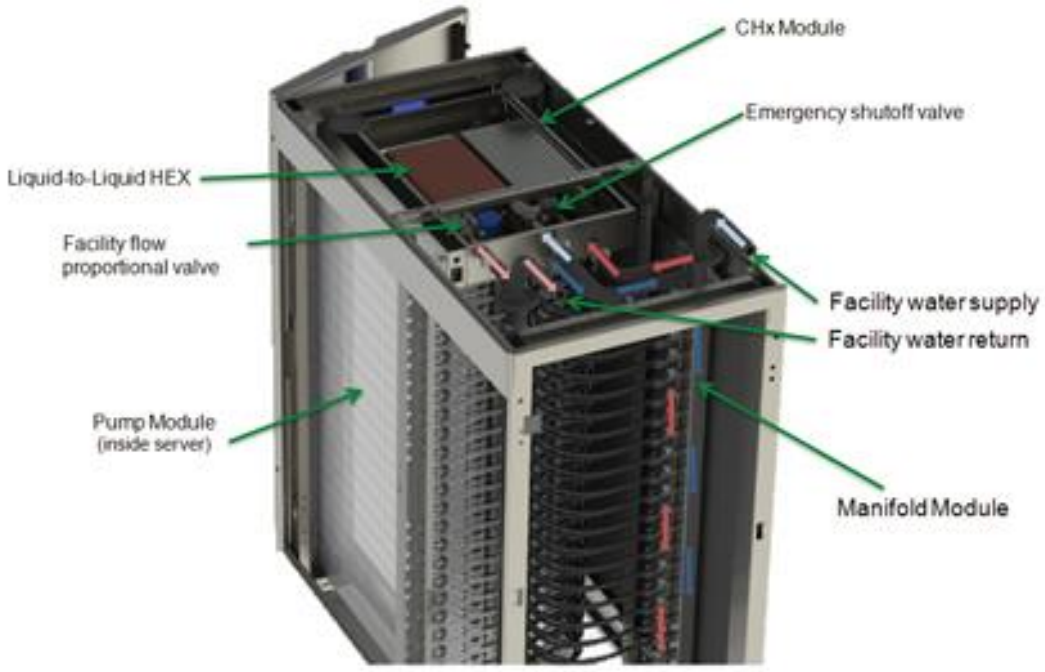

Figure 1-2 Main elements of the Direct Liquid Cooling System (DLCS) [2]

Fluid Medium	Heat Capacity (J/g^{O}C)	Conductivity	Kinematic Viscosity
Air	1.01	0.02	0.16
Dielectric mineral oil	1.67	0.13	16.02
Water	4.19	0.58	0.66

Table 1-1 Comparison of Different Cooling Medium [11]

1.1 Scope of the Work.

The proposed effort is divided into four sub-tasks. Firstly, a reference chip module platform as shown in Figure 1-3, is designed and manufactured. Careful consideration is paid to dimensional and power consumption constraints involved in employment of these devices in the solution. A bench setup is implemented to mount the cold plates on the chip module which serves to provide the delivery of coolant to different parts of the chip module based on the amount of heat being dissipated in adjoining active regions. Generating the cooling circuit and selection of heat transfer surfaces within the body of the solution are also required exercises. The second sub-task involves studying the steady-state performance of the solution to determine its range and sensitivity. Followed by the cold plates performance is studied by analyzing the pressure drop and temperature change across the cold plate. Also, the base thermal resistance of the cold plate is determined to improve the optimum performance the cold plate. The final sub-task is to implement a bench setup to host any cold plate and to study its performance.

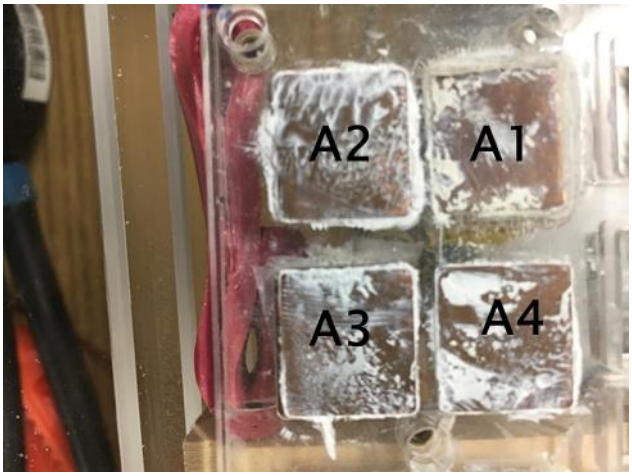

Figure 1-3 Chip Module with one section

Chapter 2

Literature Review

The emergence of Liquid Cooling in thermal management of electronic devices has been studied in various literature. Tuckerman and Pease [3] experimented the idea of cooling a chip by forcing coolant through the closed channels etched on the backside of the silicon wafer. They also reported that, the heat transfer coefficient is inversely proportional to the channel width in case of a laminar flow. This idea has influenced various researchers working in the design and optimization of heat sinks, especially for electronics. Zhang et al. [4] stepped further by experimentally characterizing the performance of a liquid cooled heat sink populated by microchannels made of Aluminum with the dimensions of 15 x 12.2mm. This experiment was also carried out on two different chip footprints, 12 x 12mm and 10 x 10mm. Thermal resistance curves were obtained in the range of 0.44 to 0.32 ^{o}C/W for the hip footprint of 12 x 12mm and 0.59 to 0.44 ^{o}C/W for the chip with footprint of 10 x 10mm. Higher heat spreading results in higher thermal resistance for the chip with a footprint of 10 x 10mm. Both the analytical and experimental results are well matched while considering the respective thermal resistance elements.

Madhusudan et al. [5] developed a thermal resistance-based network model to characterize microchannel cooling system for electronics thermal management. Spreading/constriction resistances are developed from the model given by Lee et al. [6]. This literature based thermal resistance model predicted that the thermally optimal design can dissipate 24% more than the practical design thus addressing the manufacturability gap. Experimental and numerical investigation of liquid cooled heat sinks containing microchannels were carried out by Chiu et al. [7] by varying the porosity, aspect ratio and imposed

pressure drop. It was reported that the Nusselt number decreases with increasing aspect ratio. The heat transfer enhancement due to the rising pressure drop is significant on microchannels with thigh aspect ratio and hence thinner channels are reported to be advantageous.

Seaho et al. [8] experimentally investigated two different design concepts of water cooled cold plates namely drilled type and tube type. This design allows the water passages through complex electronic package structure. Heat transfer coefficient values are reported in the range of 6000-17000 W/m^2K for a flow rate of 0.5-1.5gpm for the tube design cold plate compared to a heat transfer coefficient value of 7000-27000 W/m^2K for a drilled design cold plate. A lighter cold plate with minimal manufacturing cost and lower pressure drop can be achieved using the tubular design. An attempt is made in the current study to characterize a cold-plate with a novel microchannel structure and flow pattern. The commercial cold-plate under investigation uses an impinging jet flow. Experiments were conducted without the impinging jet flow and by varying the flow rate and inlet power while maintaining the coolant temperature at 20°C. Heat transfer coefficient values were calculated from the obtained base thermal resistance and the literature-based relations. The temperature rise across the cold plate is measured for various coolant flow rate and chip power, the pressure drop across the cold plate is studied by varying the flow rate and keeping input power constant.

Chapter 3

Copper Heater Blocks to mock a High Powered Electronic Package

For this experimental study, a reference platform is required to design a high powered electronic package. Figure 1-3 shows a section of the high-power chip module, provided by Endicott Interconnect Technologies Inc. (now i3 Electronics, Inc.), that serves the purpose. This module is populated with an array of heat generating component such as Application Specific Integrated Circuit (ASICs) and setup to have maximum power distribution of 480W. These ASICs are 14.71 x 13.31 x 0.8mm in size. A copper heat spreader, designed to account for disparity in component heights and spreading of heat, is not considered in this study to take advantage of multiple spatially- separated heat sources on the chip module.

For the purpose of this study, the cold plates mounted on high-power density chip modules and the schematic of the setup is shown in Figure 3-1. The setup consists of an array of heater blocks to mock a server chip. Thick film heaters of dimension 12.7 x 12.7mm are soldered to the base of copper blocks to simulate the ASICs. A hole was drilled midway into the side of each block such that the attached thermocouples measures temperature 1mm below the center of the top surface. These measurements are intended to represent case temperatures of ASICs.

The base of the chip module was machined from acrylic consisting two parts to hold the heater blocks. The top half ensures that the installed heater blocks only extend 0.8mm above the base while the bottom half prevents the heater blocks from moving when either cold plate is attached with applied pressure. The holes in the bottom half of the base facilitate exit of heater leads and thermocouples from individual heater block.

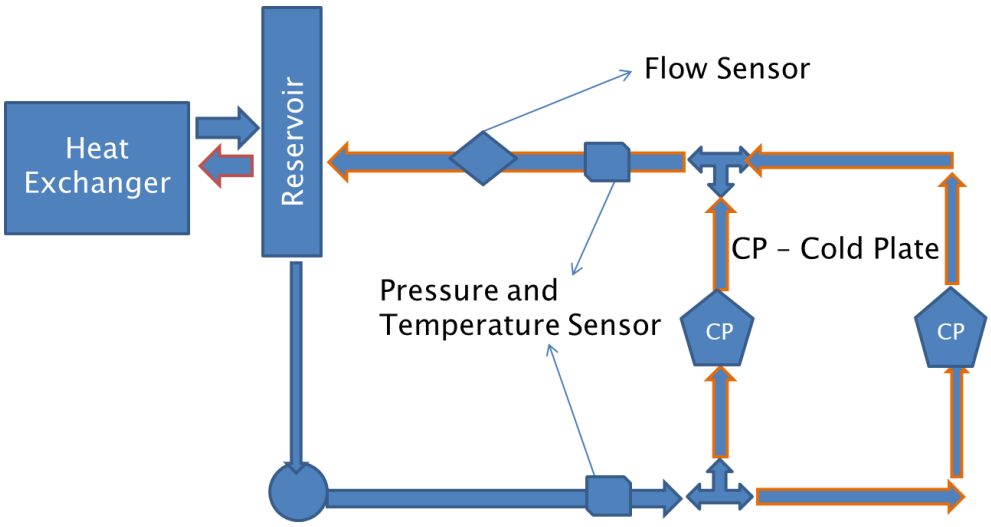

Figure 3-1 Schematic of Experimental Setup

Controlling power dissipation of each heater block is achieved like details in Figure 3-2. the current drawn by the heater blocks are measured with the help of a shunt resistor based on the voltage drop readings through the data acquisition unit (DAQ). A board with eight individual circuits were assembled for blocks in Sections A and B. Each section is populated with four heater blocks and were named starting from the top right and moving in a 'C' pattern. Both sections have a similar footprint and account for maximum power dissipation of 240W.

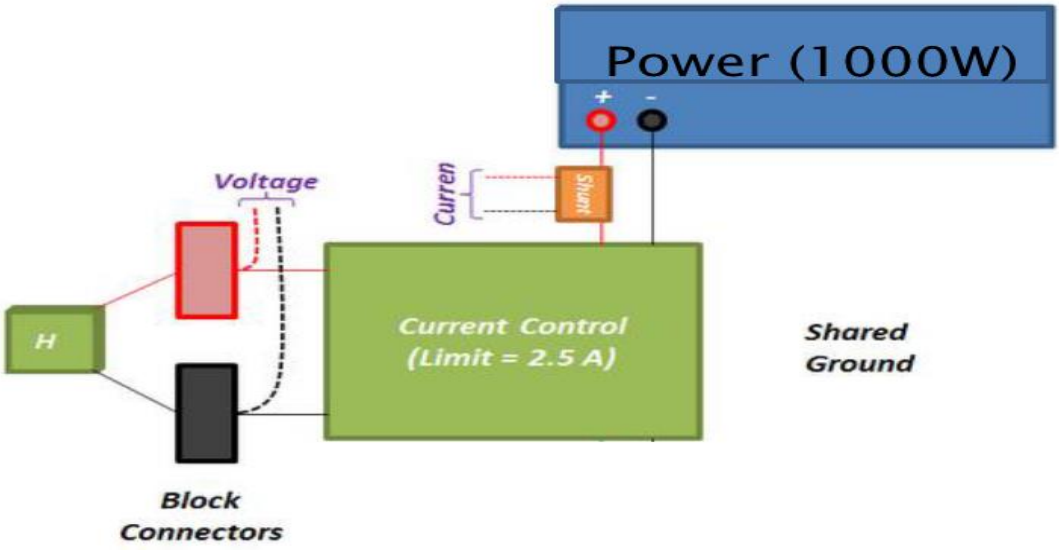

Figure 3-2 Block Diagram of a Single Heater Control Circuit [13]

Chapter 4

Cold Plate Mounting

The experimental facility is built in-house to achieve high accuracy measurements, and it includes building a mock chip, taking measurements on the base of the cold plate, assembling the cold plate to the mock server (copper block) and a sanity check for air voids at the Thermal Interface Material (TIM). Figure 4-1 shows the cold plate used for this study. The cold plates are used in Asetek Rack D2C to the purpose of accommodating lower profile footprints such as custom chases. The cold plate employs microchannels with a split-flow technology as a solution to decrease the cold plate thermal resistance. The cold plate consists of two main parts; the plastic cover part to provide the required impinging flow to the copper part with microchannels. The fin area is 31.6 x 26mm with a fin pitch of 0.23um and fin thickness of 0.11um.

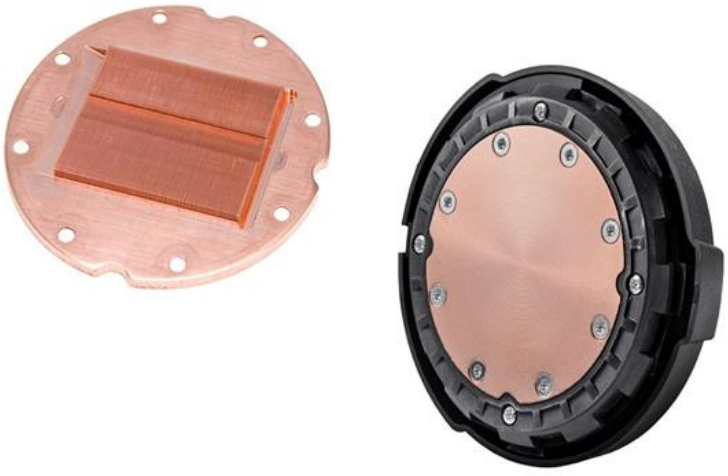

Figure 4-1 Asetek Cold Plates [19]

Meticulous care was taken in assembling the cold plate on the heater block as uneven assembly would lead to formation of air voids at the interface, which would lead to non-uniform power distribution. A syringe was used to evenly dispense the TIM over the heater block, as shown in the Figure X. The cold plate assembly on top of the heater block was done in multiple steps.

Chapter 5

Experimental Test Setup

The control scheme was designed in LabVIEW to characterize the cold plate by studying the parameters such as temperature, pressure and flow across the cold plates. The mock chip module as mention earlier was designed and fabricated for the experimental testing. Details of liquid cooling rest bench are also finalized and previewed. Finally, a series of tests are conducted on both cold plates and resultant parameters of interest are outlined.

5.1 The Centralized Pump

The selected Swiftech MCP50X pump as show in Figure 5-1, has pulse width modulated (PWM) control so it can be used to control the flowrate of distilled water (Coolant). This pump has a smaller footprint and higher-pressure head capacity with low power requirement. It works on centrifugal pumping mechanism and operates really at low noise. It is powered by a DC supply through a SATA cable and has a 4-wired connector for PWM control. Also, the pump has an attached reservoir with a standard G1/4" ports which are compatible with large assortment of fittings. The PWM enables control of speed of the flow through an Arduino, for a wide range of speeds, from 1200 rpm for a silent operation to 4500 rpm for an ultra-high flow performance.

Figure 5-1 Swiftech MCP50X Pump [16]

5.2 Flowmeter

The Omega FTB-421 flowmeter was selected as it has range of operation from 0.1 to 2.5 lpm. It has an accuracy of +-3% of reading normal range and repeatability of 0.5% FS normal range. The flowmeter accuracy and repeatability were checked by recalibrating the flowmeter frequently. The lightweight turbine ensures fast startup and can mount in any orientation.

Figure 5-2 Omega FTB-421 Flowmeter [18]

5.3 Pressure Sensor

The pressure sensors selected is Honeywell MLH050PGL06E which works on silicon Piezo-resistive pressure sensing principle. The pressure sensor is equipped with four piezo-resistors suppressed in a chemically- etched silicon diaphragm. This diaphragm is being flexed together with the suppressed resistors whenever there is a change in pressure that induces stress. This results to an electrical output when the resistor value changes in proportion to the stress applied. These sensors were selected as they are small, more reliable and cheap. They report maximum repeatability, precision and reliability under different conditions. Also, they are highly consistent regarding operating characteristics and interchanges without recalibration.

Figure 5-3 Honeywell MLH050PGL06E Pressure Sensor [17]

5.4 Thermocouple Probe

The thermocouple probes from OMEGA are selected as they have quick disconnect with miniature connectors. The glass filled nylon connector is rated for temperatures up to 220°C. The diameter of thermocouple probe is 3.0mm. These thermocouple probes are fitted into stainless steel vacuum fitting as shown in Figure 5-4 (b). The vacuum fittings are then fitted into fluid line by use of Tee joint.

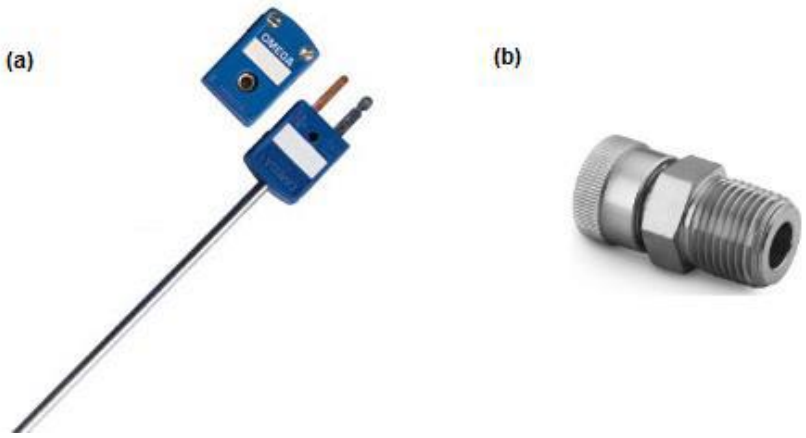

Figure 5-4(a) Thermocouple Probe (b) Vacuum Fitting

5.5 Data Acquisition Units (DAQ)

The Agilent 34972A DAQ unit has a 3-slot mainframe with built-in 61/2-digit DMM and eight optional switch and control plug-in modules. It measures and converts 11 different input signals: temperature with thermocouples, RTDs and thermistors; dc/ac volts; 2- and 4-wire resistance; frequency and period; dc/ac current. In stand-alone applications during the experiment, the temperature rise in heater blocks were instantaneously logged onto a USB flash drive. The Bench Link Data Logger software was used for logging data and controlling the process in the stand-alone mode.

Figure 5-5 Data Acquisition Unit (DAQ) [15]

Chapter 6

Liquid Cooling Test Bench

A simplified sketch of the test bench setup to evaluate both cold plates is depicted in Figure X. A Kinetics RS33AO11 recirculating chiller drives flow through the external loop and cools the plate heat exchanger (HEX). The chiller is equipped with a positive displacement pump capable of pumping up to 1.6gpm of coolant at 100psi and a temperature range of -15°C to 75°C. As these units are known to drift (variation in temperature), the HEX provides substantial thermal capacitance to prevent transmission to subsequent loops. A DC 4-wire pump drives flow of distilled water through the two HEXs in the intermediate loop. Similarly, a separate pump controls flow of distilled water through all components in the internal loop. Turbine flow-meters measure the flow rate of water cooled by the plate HEX. Temperature and pressure differences across the cold plate are measured using T-type thermocouple probes and pressure transducers. The pump in the internal loop is primarily responsible for maintaining a fixed flow rate during testing. The pump in the intermediate loop controls the inlet temperature of water to the cold plate by modulating flow rate between the two HEXs. Temperature and flow rate readings are input to the LabVIEW code that in-turn controls both pumps by sending PWM signal through Arduino. Inlet temperatures to the cold plate is relatively high (35°C) to test for warm water cooling. Water and glycol mixture (50/50) is employed in external loops to have effective running of chiller. The Agilent 34970A Data Acquisition/Switch Unit is used to sense temperature, pressure, flow, voltage and current by compiling a LabVIEW program. There are thirteen case temperature readings measured from the MCM as mentioned in section 4.1 through the LabVIEW program. Agilent E3632A 120W power supply is used to power the pressure sensor, flowmeter. A Corsair CX750M power supply unit is used to power the 4-wired DC pumps since they have a SATA cable.

6.1 Experimental testing of Cold Plate

The experimental test setup was operated at an inlet temperature of 20oC which the safest operating region for the chip modules even at high power running. The chip modules were subjected to uniform loading conditions during the testing of the liquid cold plate. There were six cases of uniform loading considered where all eight ASICs were subjected to uniform loads of 10W, 20W, 30W, 40W, 50W and 60W. All the loading conditions were studied at different flow rates varying the PWM from 50 to 100 in the internal loop. Two flowmeters were used in parallel to make sure the flowmeter operates in its working range. The pressure drop across the cold plate is measured and utilized to calculate the pumping power.

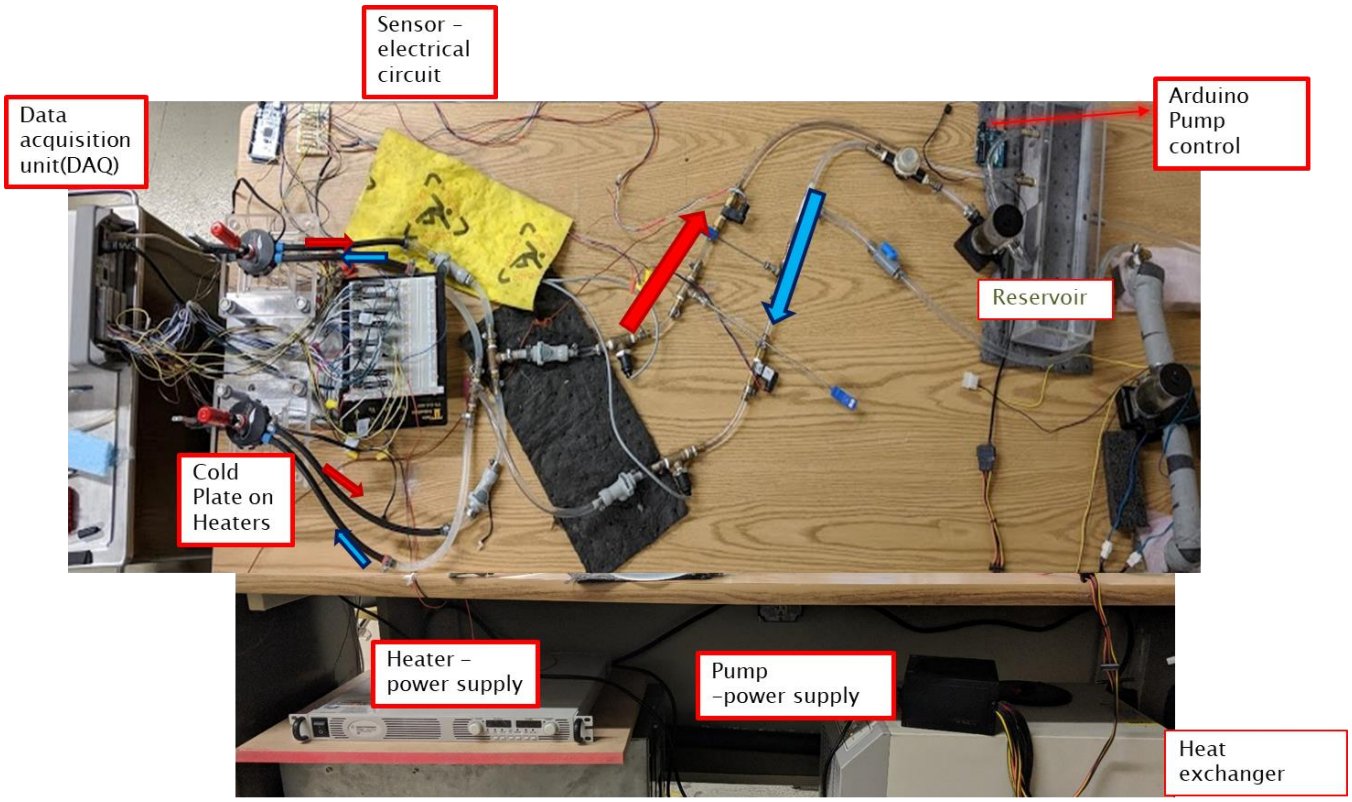

Figure 6-1 Experimental Bench Setup

The LabVIEW code has been written and the data are monitored instantaneously using the Agilent Bench link Software as shown in Figure X. The PWM signal to the pump are controlled by the LabVIEW program as shown in Figure X. The base temperature is an important measurement to be determined with accuracy. The value depends on the geometrical shape and on the total amount of energy to be dispersed. A 1mm hole was drilled beneath the heater block and a T-Type Thermocouple is placed inside to measure the base temperature. T type thermocouples were calibrated using a precision oven by varying the oven temperature from room temperature to 45oC.

(a)

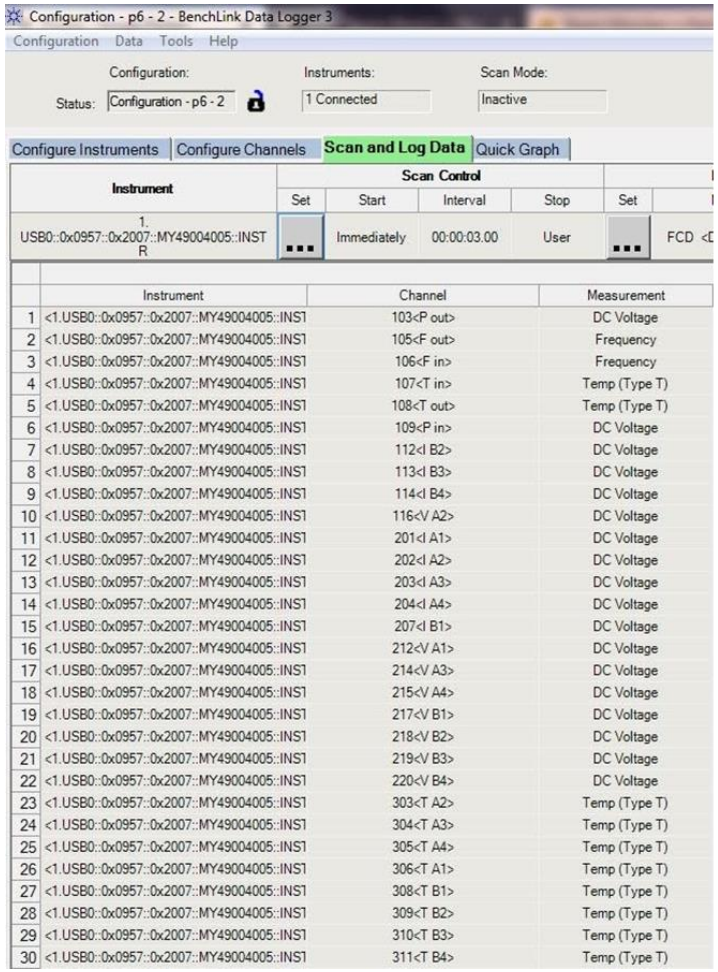

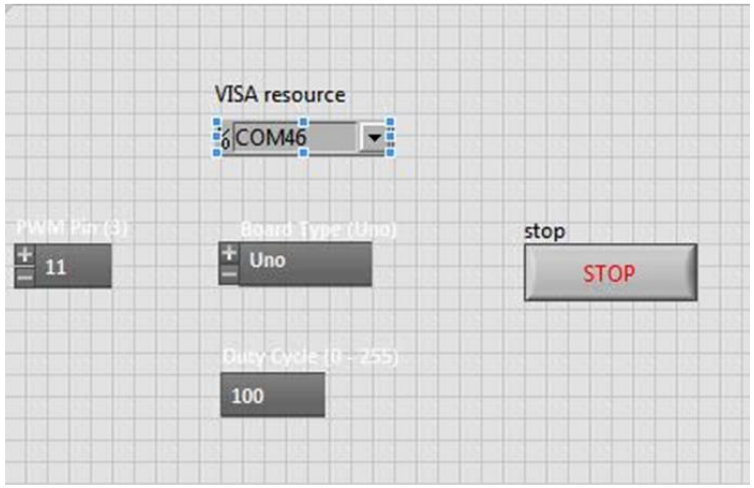

Figure 6-2 (a) Agilent Bench Link Data logger (b) LabVIEW Front Panel

Chapter 7

Results

7.1 Temperature profile of the heaters.

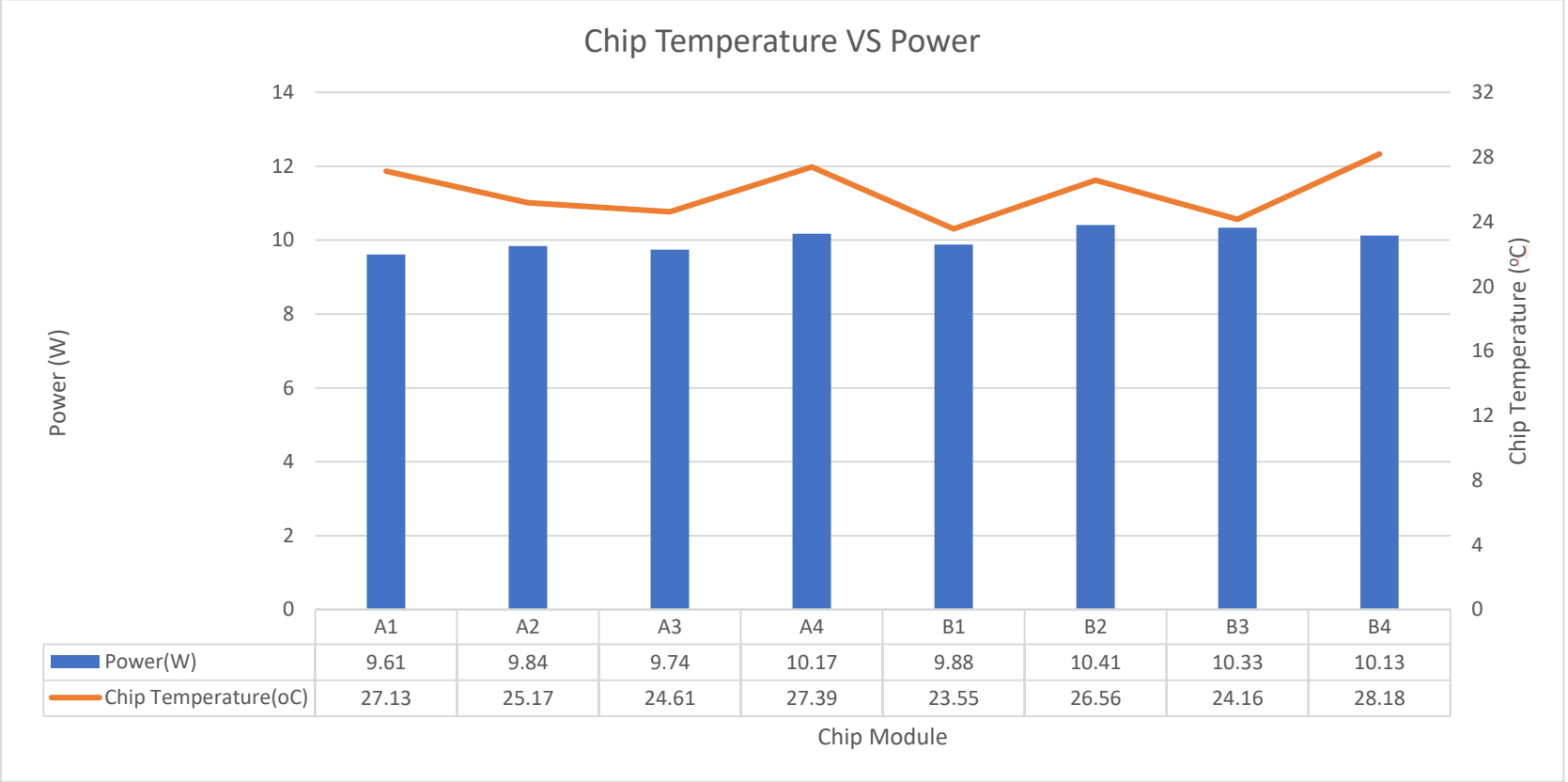

Figure 7-1 Temperature Profile of the Heaters

Firstly, the threshold temperatures of heater blocks are determined to have a safe operating region. The inlet temperature is maintained at 20^{o}C using the Kinetics RS33AO11 recirculating chiller devices and the maximum flow rate is allowed through the water circuit. The pump PWM is given a duty cycle of 100 which generates a flowrate of 0.89lpm through the coolant circuit loop. Figure 7-1 shows the plot of Chip Temperature against the Power supplied to the heater blocks. Although, a constant power of 10W is supplied to each heater block, there is a deviation in the power pulled by each heater block, which is due to the resistance change in resistors. Every resistive heater is measured using a multimeter for its resistance and there is an offset found on each resistor before operating.

7.2 Temperature difference as a function of coolant inlet temperature

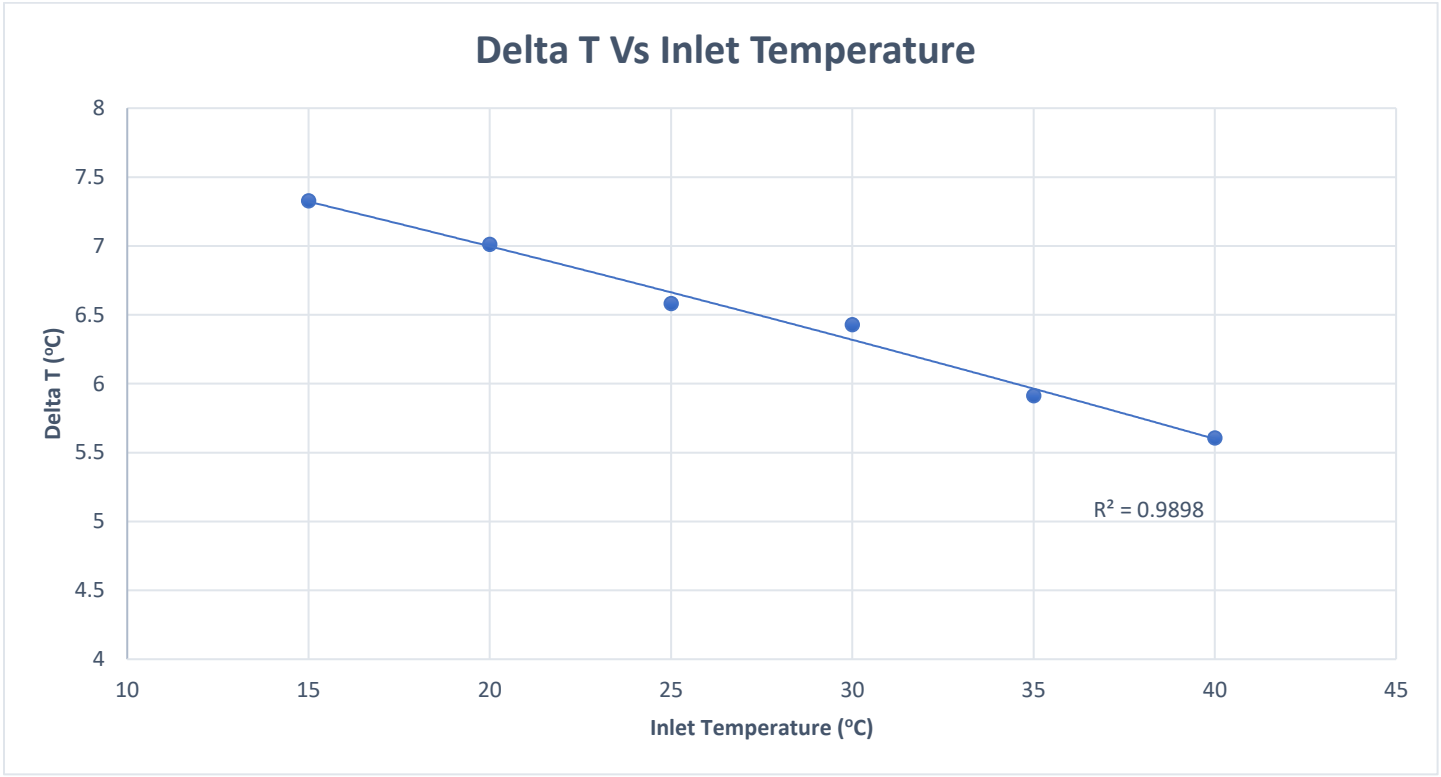

Figure 7-2 Temperature Difference as a Function of Coolant Inlet Temperature

The change in temperature across the cold plate is monitored by varying the inlet temperature using the Heat exchanger. The input power to both sections of the heater blocks are maintained at 320W and a constant flow rate of 0.89lpm is set thus the water flow constant in the loop. The Figure 7-2 shows a linear decrease in the temperature rise as the inlet temperature increases. This plot satisfies as a trend value of 0.9898 is observed to the linear polynomial curve.

7.3 Pressure gradient at various flowrates

To validate the energy equation, the pressure gradient across the cold plate is studied in the same fashion by keeping the input power constant at 320W and maintaining the coolant inlet temperature to the cold plate at 20^{o}C. The plot shows a linear increase in the change in pressure as the flow rate increases. The flow rate is varied by controlling the PWM signals. This satisfies the energy equation

$$Q = mCp\Delta T$$

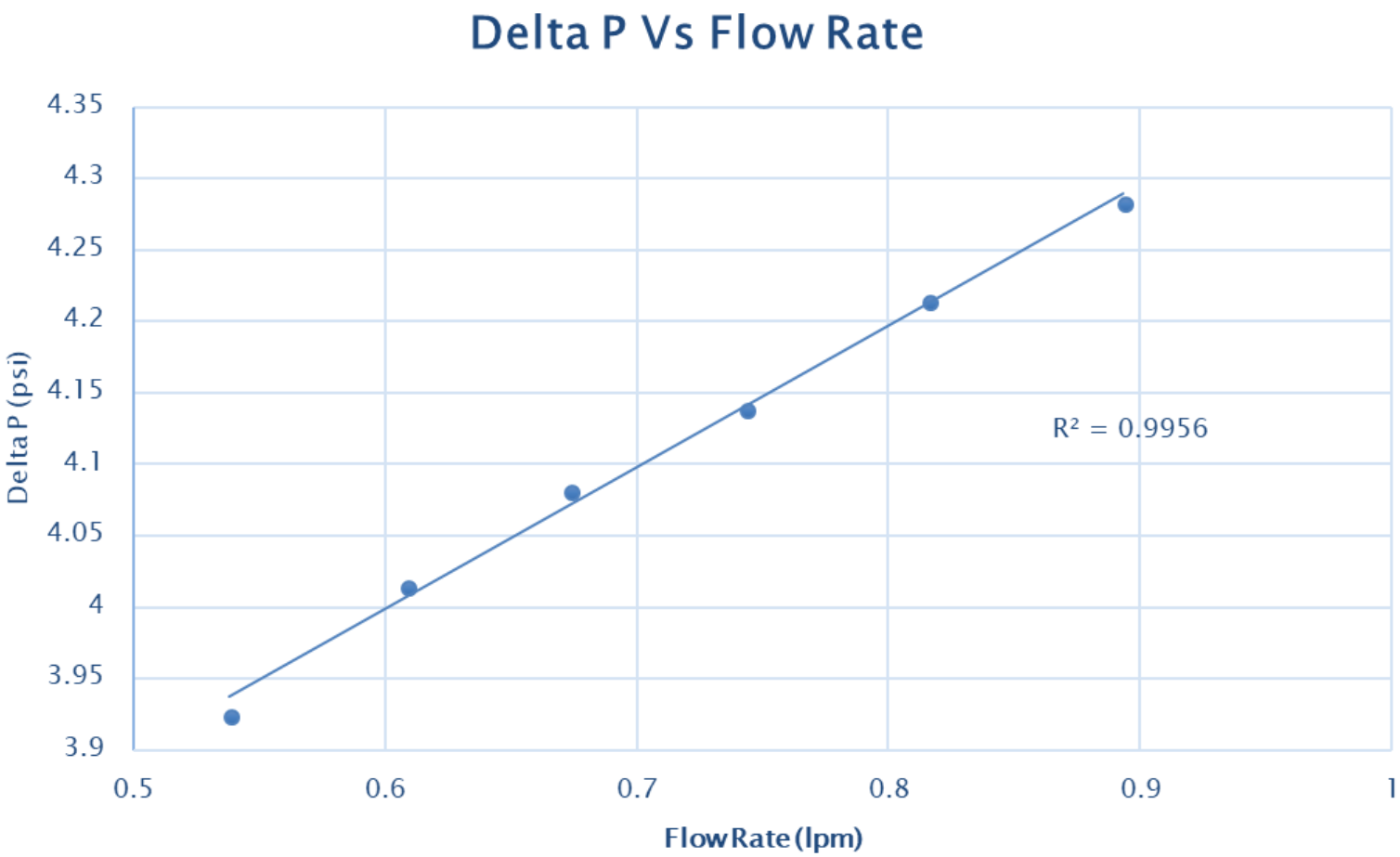

Figure 7-3 Pressure Gradient at Various Flowrates

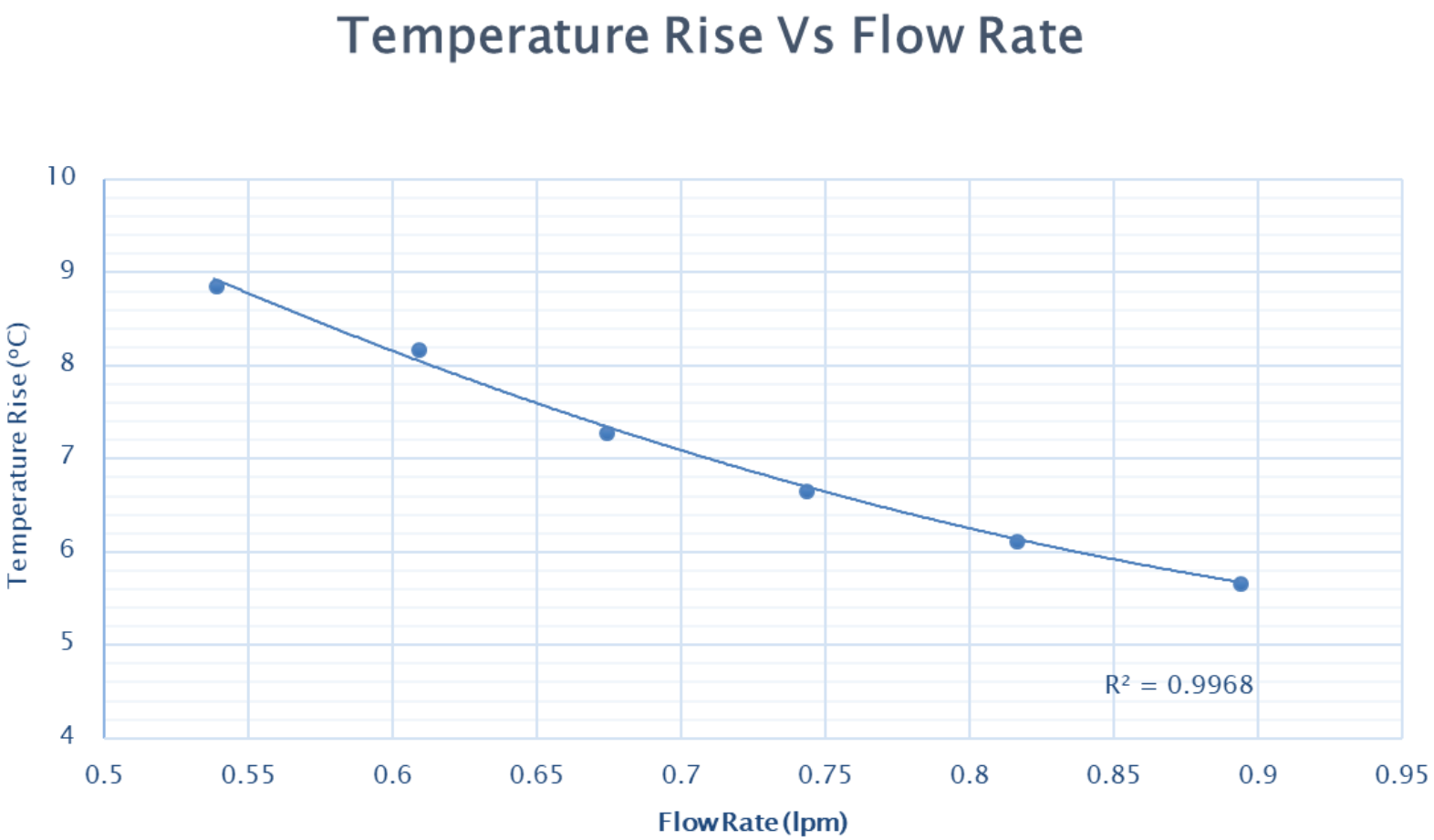

Figure 7-4 Temperature Gradient at Various Flowrates

7.4 Temperature gradient at various flow rates

The change in temperature across the cold plate is studied by varying the flow rate and having the input power and the inlet temperature constant. The input power to the heater blocks is the same as previous which is 320W and the inlet temperature is maintained at 20^{o}C. The trend line value of 0.9968 of quadrilateral polynomial is observed in this case. The plot is shown in Figure 7-4.

7.5 Thermal resistance calculation

The thermal resistance is calculated by the following formula. The inlet temperature of the coolant is maintained at 20^{o}C and the maximum flow rate is allowed through the coolant circuit. The input power to the setup is varied and the thermal resistance is calculated.

$$R_{TH} = \frac{T_b - Tin}{Q_{in}}$$

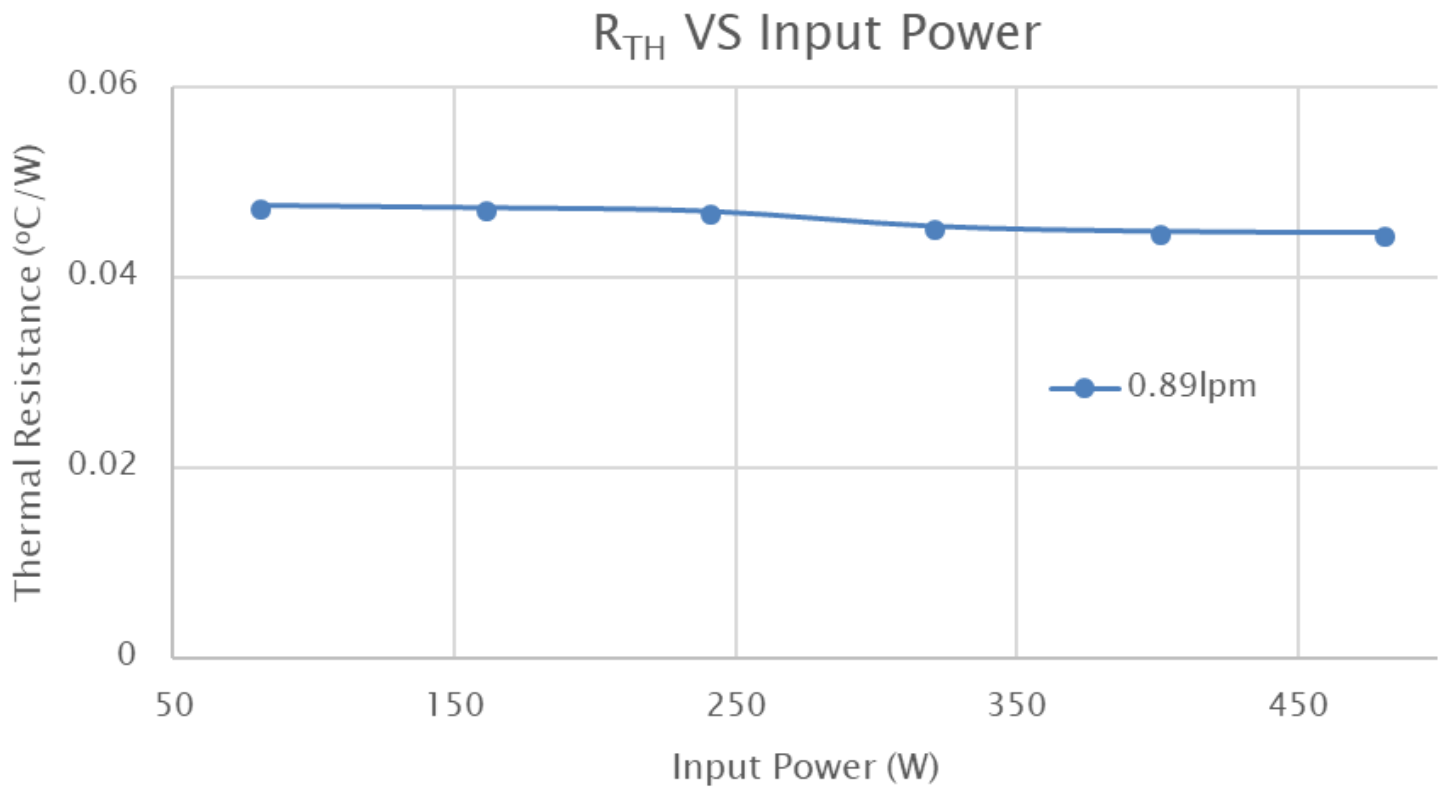

Figure 7-5 Thermal Resistance Plot

Chapter 8

Flow Control Device

8.1 Flow Control Device Schematic

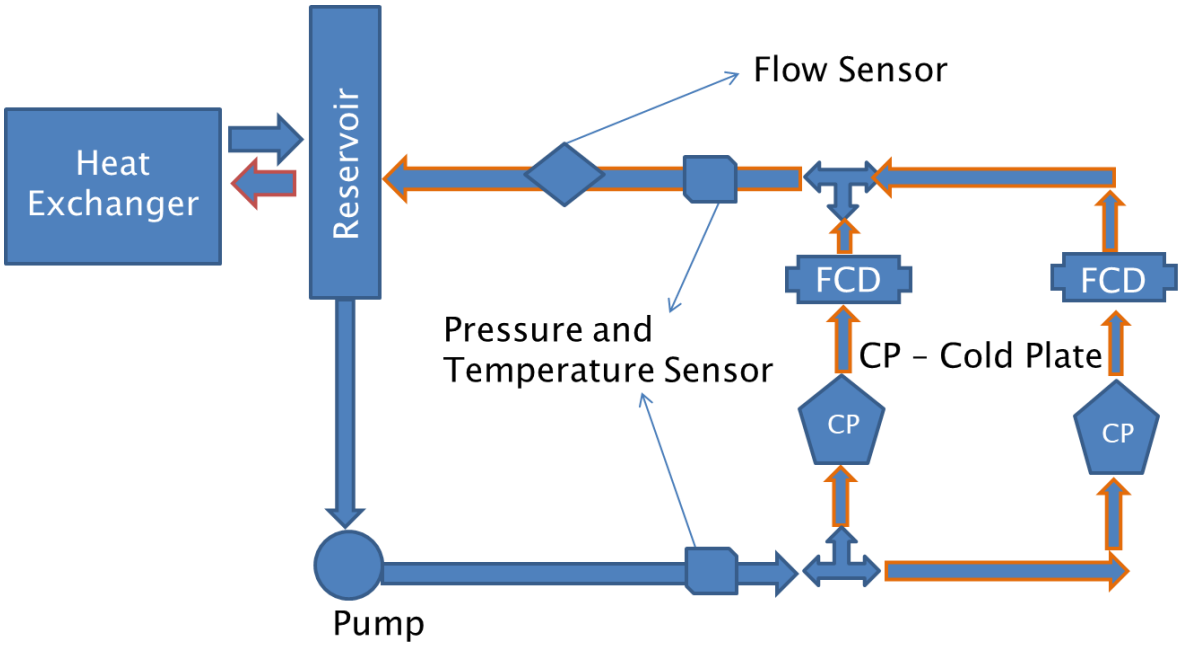

Figure 8-1 Schematic Diagram of a Flow Control Device in the circuit

A flow control device (FCD) is installed at the exit of each cold plate to regulate the flow through the circuit. These are self-regulating FCDs based on the temperature change in the coolant. The FCDs must be place closer to the exit of the cold plate to avoid response time. Also, the maximum performance can be achieved by placing the FCDs closer to the cold plate as shown in Figure 8-1.

8.2 Power Savings with FCD

The performance characteristics of the FCD are studied by connecting them in the coolant loop without cold plate and heater blocks and an optimum working range is obtained. The Figure 8-2 shows the experimental test results of the FCD connected in the coolant circuit. Also, the plot of change in temperature against the inlet temperature is considered, where the inlet temperature of 35^{o}C give us a change in temperature of 6^{o}C. An inlet temperature of 35^{o}C is considered as we are dealing with warm water cooling.

Comparing that data with the FCD experimental setup, it is clearly seen that there is a variation in flow rate from 1.03lpm to 1.09lpm. These calculations are carried out for a 160 W power module and a pump savings of around 5.82% is calculated. By increasing the modules, the use of FCDs increases at the exit of the cold plates which results is more pumping power savings.

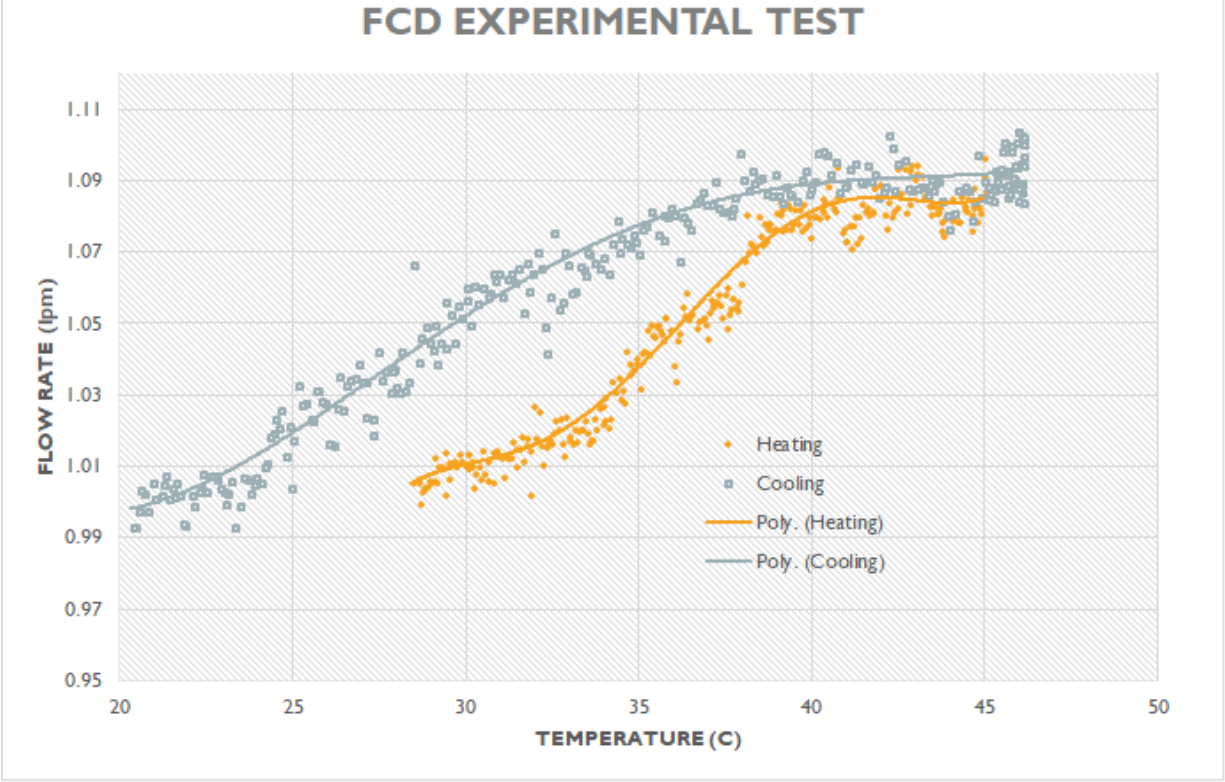

Figure 8-2 Experimental Results of Flow Control Device

Chapter 9

Conclusions

A test rig was designed and built to characterize the cold plate of interest. Characterization of cold plate was done by performing thermal resistance experiments by changing the coolant flow rate and chip power. Cold plate thermal resistance values were calculated with minimal percentage deviation with respect to input power. It was also observed that the cold plate thermal resistance decreases with flow rate. Higher flow rates can be obtained at the price of higher pressure drop. A chip module with bisection is designed and fabricated to produce a power of 480W together. Specifics of cost-effective design and fabrication of a mock chip module were outlined. Control circuits that enabled automation of testing through modulation of heaters and cooling systems were demonstrated with a simplified test setup.

A close approximation of heat transfer coefficient was then obtained from the measured cold plate thermal resistance values and a well established thermal resistance values can be lowered, in other words, the heat transfer coefficient values can be improved with a much-improved design of the heat sink. The installation of FCDs at the exit of the cold plate results in more pump power savings. The centralized pump instead of an impinge inside the cold plate results in more savings.

Chapter 10

Future Work

A bench setup with a universal mounting technique to mount any cold plate of interest should be developed. Mounting of cold plate on the heater block can be carried out by improved mounting techniques. Cold plates are characterized in parallel circuit. Series connection of cold plates should be characterized and comparison of both must be studied. The cold plate thermal resistance values can be lowered with much improved design of the heat sink.

Appendices

Appendix A

Computational Fluid Dynamics

The equations that govern the motion of a Newtonian fluid are the continuity equation, the Navier-Stokes equations, the momentum equation and the energy equation. The set of equations listed below represents seven equations that are to be satisfied by seven unknowns [3]. Each of the continuity, energy, and momentum equations supplies one scalar equation, while the Navier-Stokes equations supply three scalar equations. The seven unknowns are the pressure, density, internal energy, temperature, and velocity components. The scope of our analysis predominantly lies in the laminar region of flow owing to low flow velocities and relatively simple geometries. The only instance where a k-Epsilon turbulence model is used is in the region between when the damper is completely closed and when it is open by an angle of 10 degrees. The equations used for solving in the laminar as well as turbulent regions are listed below.

$$\text{Continuity}: \quad \frac{\partial \rho}{\partial t} + \vec{\nabla} \cdot (\rho \vec{u}) = 0$$

$$\text{Momentum}: \quad \rho \frac{D\vec{u}}{Dt} = -\vec{\nabla} p + \nabla(\mu \nabla \vec{u}) + \vec{f}_b$$

$$\text{Energy}: \quad \rho \frac{DE}{Dt} = -\vec{\nabla} \cdot (p \vec{u}) + \vec{\nabla} \cdot \left(k_t \cdot \vec{\nabla}(T)\right) + \Phi + S_E$$

$$\text{Turbulent kinetic energy}: \quad \frac{\partial(\rho k)}{\partial t} + \vec{\nabla} \cdot (\rho k \vec{u}) = \vec{\nabla} \cdot \left[\alpha_k(\mu + \mu_t) \cdot \vec{\nabla}(k)\right] + 2\mu_t E_{ij} \cdot E_{ij} - \rho\varepsilon$$

$$\text{Turbulent dissipation}: \quad \frac{\partial(\rho \varepsilon)}{\partial t} + \vec{\nabla} \cdot (\rho \varepsilon \vec{u}) = \vec{\nabla}\left[\alpha_\varepsilon(\mu + \mu_t) \cdot \vec{\nabla}(\varepsilon)\right] + C_{1\varepsilon}^{*} \frac{\varepsilon}{k} 2\mu_t E_{ij} \cdot E_{1j} - C_{2\varepsilon}\rho \frac{\varepsilon^2}{k}$$

where

$$\mu_t = \rho C_\mu \frac{k^2}{\varepsilon}, \quad C_\mu = 0.0845, \quad \alpha_k = \alpha_\varepsilon = 1.39,$$
$$C_{1\varepsilon} = 1.42, \quad C_{2\varepsilon} = 1.68$$

and

$$C_{1\varepsilon}^{*} = C_{1\varepsilon} - \frac{\eta\left(1 - \frac{\eta}{\eta_0}\right)}{1 + \beta\eta^3}, \quad \eta = \left(2E_{ij} \cdot E_{ij}\right)^{1/2} \frac{k}{\varepsilon},$$
$$\eta_0 = 4.377, \quad \beta = 0.012$$

Appendix B

Supplementary Pictures

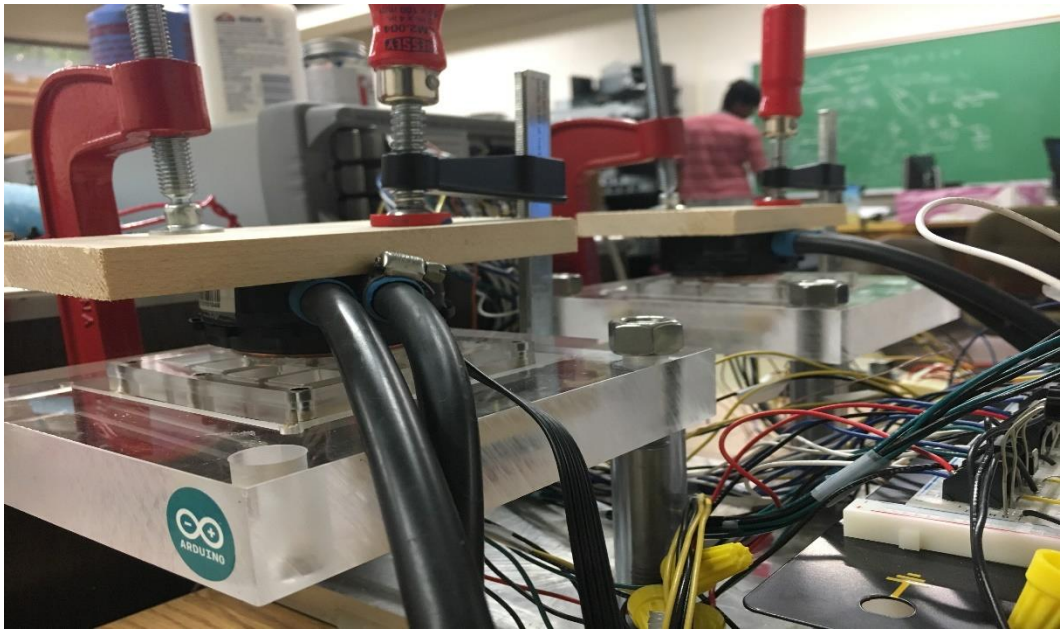

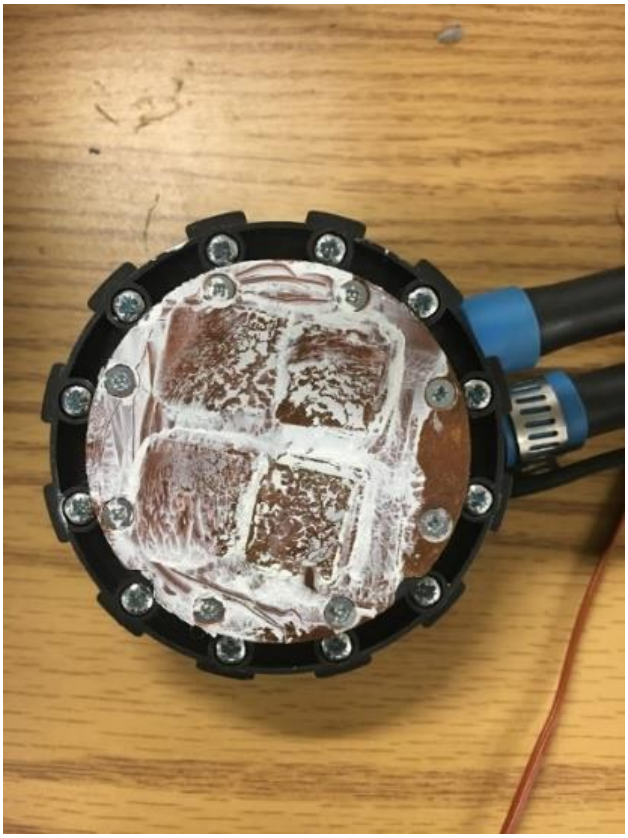

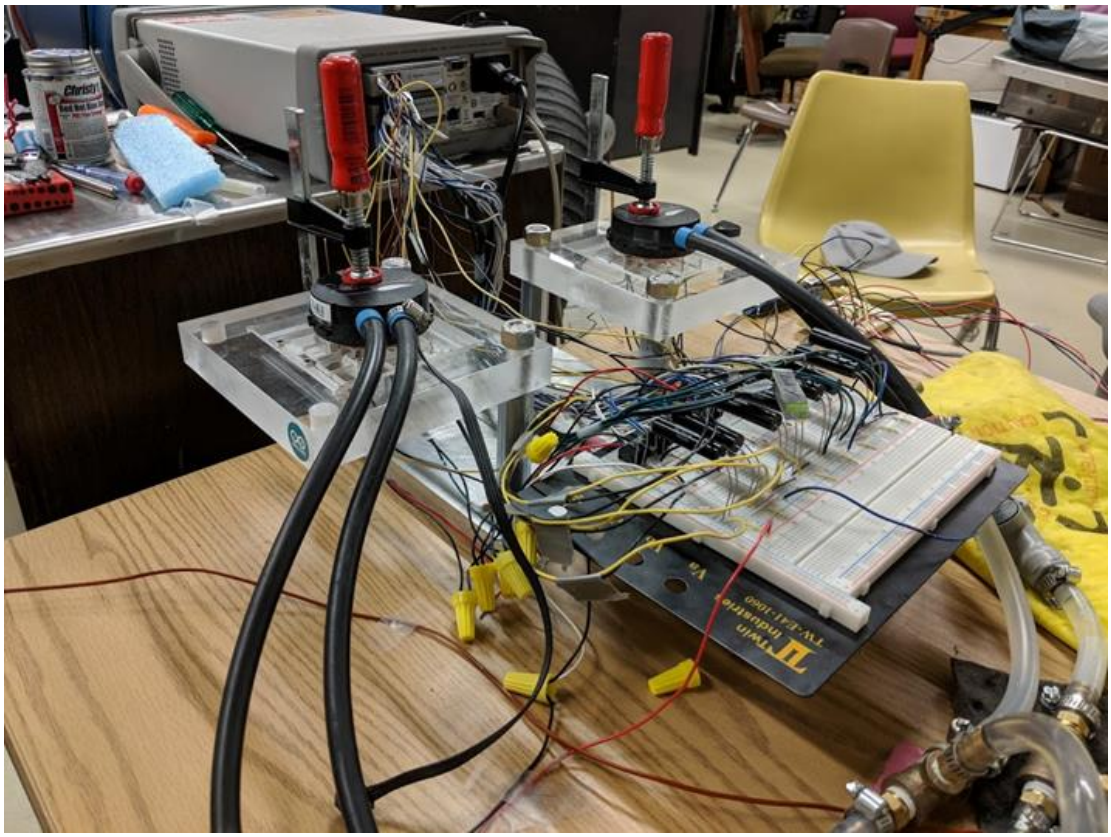

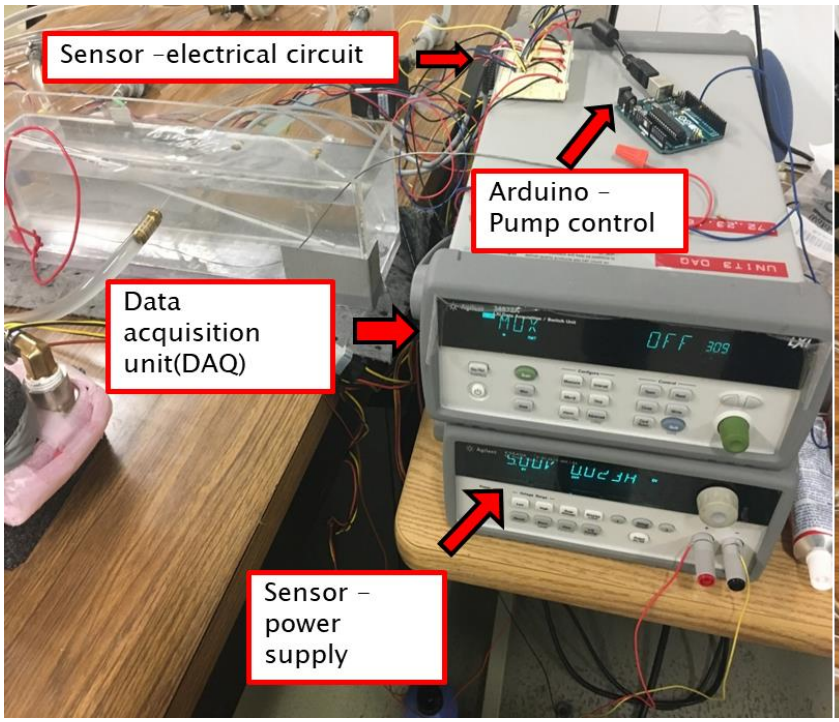
Sensor –electrical circuit
Arduino – Pump control
Data acquisition unit(DAQ)
Sensor – power supply

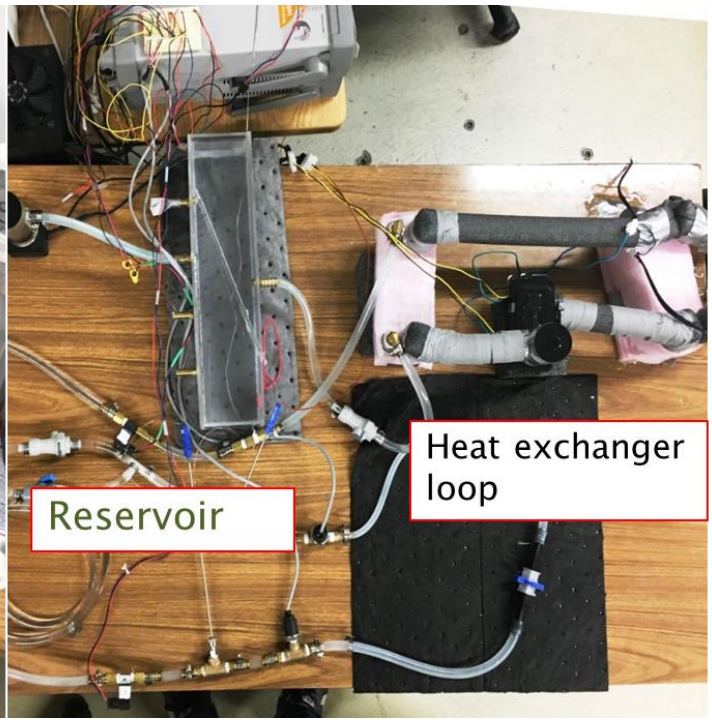
Heat exchanger loop
Reservoir

References

[1] https://www.channelpartnersonline.com/2018/02/05/att-poised-to-follow-verizons-lead-sell-data-centers/

[2] https://www.electronics-cooling.com/2012/12/direct-contact-liquid-cooling-for-the-datacenter-can-it-be-simple-low-cost-high-performance-and-efficient/

[3] D. B. Tuckerman and R. F. W. Pease, "High-performance heat sinking for VLSI," IEEE Electronic Device Lett. vol. EDL-2. DD. 126-129, May 1981

[4] H.Y. Zhang, D. Pinjala, T.N. Wong, K.C. Toh, Y.K. Joshi, "Single-phase liquid cooled microchannel heat sink for electronic packages", Applied Thermal Engineering, Volume 25, Issue 10, July 2005, Pages 1472-1487, ISSN 1359-4311

[5] M. Iyengar and S. Garimella, "Design and Optimization of Microchannel Cooling Systems," Thermal and Thermomechanical Proceedings 10th Intersociety Conference on Phenomena in Electronics Systems, 2006. ITHERM 2006., San Diego, CA, 2006, pp. 54-62.

[6] S. Lee, S. Song, V. Au, and K.P. Moran, "Constriction/Spreading Resistance Model for Electronic Packaging", Proceedings of the 4th ASME/JSME Thermal Engineering Joint Conference, Vol. 4, 1995, pp. 199-206.

[7] Han-Chieh Chiu, Jer-Huan Jang, Hung-Wei Yeh, Ming-Shan Wu, "The heat transfer characteristics of liquid cooling heatsink containing microchannels", International Journal of Heat and Mass Transfer, Volume 54, Issues 1–3, 15 January 2011, Pages 34-42, ISSN 0017-9310

[8] Seaho, S., Moran, K. and Rearick, D. (IBM corporation) and Lee, S. (Aavid Engineering), "Thermal Performance Modeling and Measurements of Localized Water Cooled ColdPlate",

[9] J. Fernandes, S. Ghalambor, A. Docca, C. Aldham, D. Agonafer, E. Chenelly, B. Chan and M. Ellsworth, "Combining Computational Fluid Dynamics (CFD) and Flow Network Modeling (FNM) for Design of a Multi-Chip Module (MCM) Cold Plate," in ASME International Electronic Packaging Technical Conference and Exhibition, Burlingame, CA, USA, 2013.

[10] U. Hwang, K. Moran and R. Kemink, "Cold Plate Design for IBM ES/9000 TCM Electronic Modules," Advances in Electronic Packaging, pp. 75-81, 1992.

[11] J. Fernandes, S. Ghalambor, D. Agonafer, V. Kamath and R. Schmidt, "Mutli-Design Variable Optimization for a Fixed Pumping Power of a Water-Cooled Cold Plate for High Power Electronics Applications," in IEEE Intersociety Conference on Thermal and Thermomechanical Phenomena in Electronic Systems, San Diego, CA, USA, 2012.

[12] Sahini, M. (2018). EXPERIMENTAL AND COMPUTATIONAL STUDY OF MULTI-LEVEL COOLING SYSTEMS AT ELEVATED COOLANT TEMPERATURES IN DATA CENTERS. [online] Uta-ir.tdl.org. Available at: https://uta-ir.tdl.org/uta-ir/handle/10106/26950 [Accessed 26 Apr. 2018].

[13] Experimental Characterization of a Cold Plate Used in Warm Water Cooling of Data Centers - IEEE Conference Publication, ieeexplore.ieee.org/document/7896929/.

[14] Fernandes, J. (2018). Minimizing Power Consumption at Module, Server And Rack-levels Within A Data Center Through Design And Energy-efficient Operation Of Dynamic Cooling Solutions. [online] Uta-ir.tdl.org. Available at: https://uta-ir.tdl.org/uta-ir/handle/10106/25008 [Accessed 26 Apr. 2018].

[15] http://www.testequipmentdepot.com/agilent/pdf/34972a.pdf

[16] https://www.swiftech.com/MCP50X.aspx

[17] https://sensing.honeywell.com/honeywell-sensing-heavy-duty-pressure-mlh-series-datasheet-32328895-b-en.pdf

[18] https://www.omega.com/green/pdf/FTB-420.pdf

[19] https://www.asetek.com/data-center/technology/data-center-components/

Biographical Information

Barath Ragul Manimaran received his bachelor's degree in Mechanical Engineering from Amrita School of Engineering, Coimbatore, Tamil Nadu, India in 2016. In August 2016, he began his master's Degree in Mechanical Engineering at The University of Texas at Arlington. Barath Ragul joined the EMNSPC to conduct research on dynamic cold plate for multi-chip modules. His area of interest includes, Automotive and Thermal Engineering particularly IC Engines. Barath Ragul Manimaran received his Master of Science degree in Mechanical Engineering from The University of Texas at Arlington in May 2018.